RSC Advances

ROYAL SOCIETY OF CHEMISTRY

www.rsc.org/advances

Graphical abstract

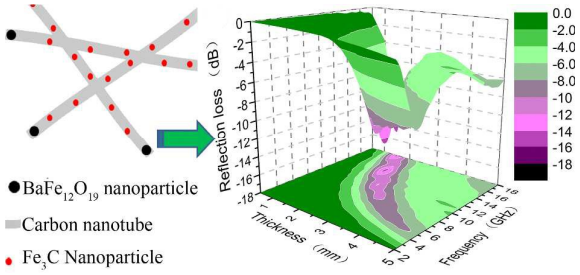

A novel kind of $BaFe_{12}O_{19}/Fe_3C/CNTs$ composite was developed by the acetylene chemical vapor deposition process. The composites perform great improvement in the microwave absorbing properties compared with pure $BaFe_{12}O_{19}$ ferrite in 2-18 GHz range.

RSC Advances

RSCPublishing

ARTICLE

Preparation and microwave-absorbing property of $BaFe_{12}O_{19}$ nanoparticles and $BaFe_{12}O_{19}$ /Fe_3C/CNTs composites

Cite this: DOI: 10.1039/xoxxoooooox

Received ooth January 2015,
Accepted ooth January 2015

DOI: 10.1039/xoxxoooooox

www.rsc.org/

Liangjun Yin[1,ξ], Tong Chen[1,ξ], Shiyu Liu[1,ξ], Yuqi Gao[1], Biao Wu[1], Yufeng Wei,[1] Gang Li[2], Xian Jian[1,*] and Xin Zhang[3,*]

$BaFe_{12}O_{19}$ ferrite was firstly prepared through a sol-gel auto-combustion process, and then $BaFe_{12}O_{19}$/Fe_3C/CNTs composites were synthesized from the acetylene chemical vapor deposition process with the introducing of $BaFe_{12}O_{19}$ ferrite at 400-600 °C. The structure and morphology of the $BaFe_{12}O_{19}$ ferrite and $BaFe_{12}O_{19}$ /Fe_3C/CNTs composites were studied using X-ray diffraction, scanning electron microscopy, transmission electron microscopy and energy dispersive X-ray. The microwave-absorbing properties of pure $BaFe_{12}O_{19}$ and such composites were investigated in the frequency range of 2-18 GHz through the evaluation of the experimental data based on the transmission line theory. The reflection loss results showed that the microwave absorption of $BaFe_{12}O_{19}$ /Fe_3C/CNTs composites performed better as the reaction temperature increasing up to 500 °C, due to the generation of the high-purity helical CNTs. The composites obtained at 600 °C performed well in electromagnetic wave loss at low frequency, owing to effective interfacial polarizations and good dispersion of magnetic nanoparticles. The composites were very potential for lightweight and strong electromagnetic attenuation materials at relatively low frequency.

Introduction

With the growing development of wireless communications, electromagnetic interference (EMI) is significantly increasing at present. All types of electric components are subject to the interference induced by electric and magnetic fields. So the microwave absorbers are the focus of extensive studies.[1-3] The suitable microwave absorbing materials own such advantages as tiny thickness, low density and wide absorbing bandwidth. Among the various microwave absorbers, the ferrite has attracted considerable attention due to its advantages of low cost, high stability and the excellent magnetic loss properties.[2] It is well-known that M-type barium ferrite ($BaFe_{12}O_{19}$) is a high performance permanent magnet.[3] It has been extensively studied owing to its fairly large magnetic crystalline anisotropy, high Curie temperature, relatively large magnetization, high resistance, low cost, excellent chemical stability, corrosion resistivity and so on. [4, 5]

Materials with dielectric loss and magnetic loss are considered to be suitable EM wave absorbers.[6] However, for $BaFe_{12}O_{19}$, due to its poor dielectric losses and fairly strong magnetic loss, which leads to poor matching of the dielectric loss and magnetic loss.[7] Then the mismatch further makes a poor microwave absorbing properties. [8,9] Therefore, much effort has been devoted to improve the electromagnetic absorption properties of the $BaFe_{12}O_{19}$.[10]

In the field of microwave absorption, carbon nanotubes (CNTs) are reported as the high-performance absorbing materials with respect to their many advantages, such as higher specific surface area , small density, and high values of complex permittivity, etc. [11,12] So the $BaFe_{12}O_{19}$ /Fe_3C/CNTs composites are predicted to be promising for attenuating EM wave. Zhao *et al.* synthesized the $BaFe_{12}O_{19}$ /MCNTs through an in situ chemical polymerization of 3-methl-thiophene (3MT) in the presence of $BaFe_{12}O_{19}$ /MCNTs composites powders.[13]

In this paper, we report the synthesis of the $BaFe_{12}O_{19}$ /Fe_3C/CNTs composites with a simple chemical process. The effects of the reaction productions as well as the morphology and microstructure of the productions were studied. The electromagnetic absorption properties were investigated and discussed combined with experiment and simulation calculation.

Experimental

Materials

For preparing the $BaFe_{12}O_{19}$ nanoparticles, $Fe(NO_3)_3{\cdot}9H_2O$ (≥98.5%), $Ba(NO_3)_2$ (≥99.5%), citric acid (99.5%), ammonia

aqueous solution, PEG (10000) were purchased from Chengdu Jinshan Chemical Reagents Company Chengdu, China. All the received reagents were analytical grade and used without further purification.

Preparation of $BaFe_{12}O_{19}$ and $BaFe_{12}O_{19}$ /Fe_3C/CNTs composites

Firstly, 8.08g of $Fe(NO_3)_3{\cdot}9H_2O$ and 5.23g of $Ba(NO_3)_2$, in a Fe/Ba molar ratio of 12, were dissolved in 100 ml deionized water with vigorous stirring at room temperature, the mixture was then dropped into citric acid solution slowly with stirring. PH value of the solution was adjusted to 7.0 with appropriate ammonia solution, and the 20 g/L PEG (10000) solution was dropped into mixture with 30 min stirring to obtain sol. The bronzing sol was then evaporated at 80 °C in a water bath for 4 hours，after that put the sol into air dry oven at 120 °C for 20 hours to gain gel. The gel was then heated at 200 °C in muffle furnace in order to proceed self-propagating combustion reaction. Grinding precursor powder was made by the above reaction. Finally the precursor powder was burned in a stove at 850 °C for 3 hours. In a typical procedure, 0.15 g of the powder was dispersed on a ceramic plate, which was transferred to a horizontal reaction tube located inside a tubular furnace at room temperature and then heated up to a synthesis temperature(400-600 °C) with a rate of 5 °C /min under N_2. When the temperature was stabilized, C_2H_2 gas was introduced at a flow rate of 30 mL/min, for 30 min in atmospheric pressure, the $BaFe_{12}O_{19}$ /Fe_3C/CNTs composites were cooled down to room temperature in the nitrogen atmosphere furnace after the growth.

Characterization and simulation

The X-ray diffraction (XRD) patterns were obtained on a (XRD-7000X). FESEM (JSM-7600F) is used to observe the morphologies of products. HRTEM images were obtained on a JEOL-2010 transmission electron microscope. Compositional analysis was performed by energy dispersive X-ray analysis (EDX). The complex permittivity was measured by the coaxial line method at 2–18 GHz using AV3618 network analyzer. The reflection losses RL (dB) of the helical material composites were calculated according to the transmission line theory, basing on the measured data of relative complex permeability and permittivity.

Results and discussion

$BaFe_{12}O_{19}$ ferrite is prepared through an auto-combustion-sol-gel process at 200 °C into muffle furnace in Air. $BaFe_{12}O_{19}$/Fe_3C/CNTs composites are synthesized by means of catalytical chemical vapor deposition (CCVD) in the range of 400-600 °C. **Figure 1** shows the XRD patterns of the as-prepared composites samples. It can be observed that the diffraction peaks at 30.23, 32.12, 34.48, 37.56, 40.09, 42.78, 55.05, 56.92, 63.87 can be assigned to the $BaFe_{12}O_{19}$ planes of (110), (107), (114), (203), (205), (206), (217), (218), (310), respectively, which match well with the standard pattern of $BaFe_{12}O_{19}$. (ICDD, PDF file No. 74-1121). It can be observed that Fe_3C appears after the catalysis of C_2H_2 using $BaFe_{12}O_{19}$ above 500 °C. Besides, a dispersion peak is also observed, which is due to the generation of the amorphous carbon. With the temperature increasing to 600 °C, the diffraction peaks of the Fe_3C still exist while the dispersion peak changes into the sharp diffraction peaks of graphite, confirming that the $BaFe_{12}O_{19}$/Fe_3C/CNTs composites have a high graphitic level at relatively high temperature.

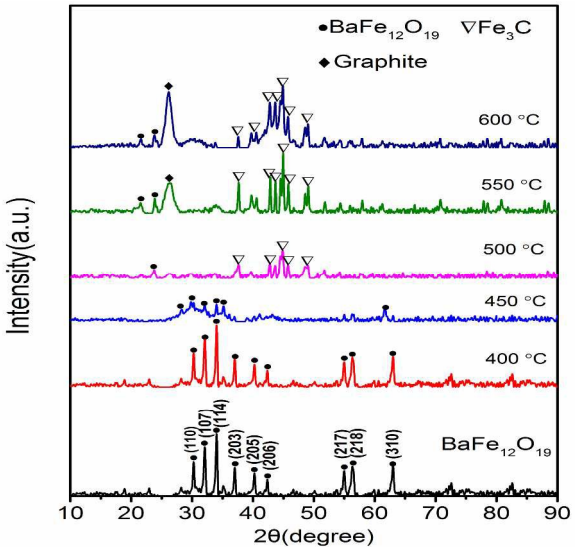

Figure 1. XRD patterns of $BaFe_{12}O_{19}$ and $BaFe_{12}O_{19}$/Fe_3C/CNTs composites synthesized at 400-600 °C.

The morphology of the $BaFe_{12}O_{19}$/Fe_3C/CNTs composites is shown in **Figure 2**. For the raw $BaFe_{12}O_{19}$ powder and composites samples synthesized at a relatively low temperature, it is observed that these samples are porous at the scale of 130-820 nm and the porous morphology doesn't change below 450 °C. Furthermore, as the temperature increasing, the as-prepared products become more compact with finny carbon nanotubes at the length of 120-280 nm. These CNTs become longer to 350-710 nm at 600 °C and have a curved morphology. From SEM observation, the reaction temperature plays a crucial role in changing the sample microstructure and CNTs content. It is demonstrated that the CNTs content increases at higher temperature resulting in the existence of graphite peaks in the 550 °C and 600 °C XRD patterns (**Figure 1**).

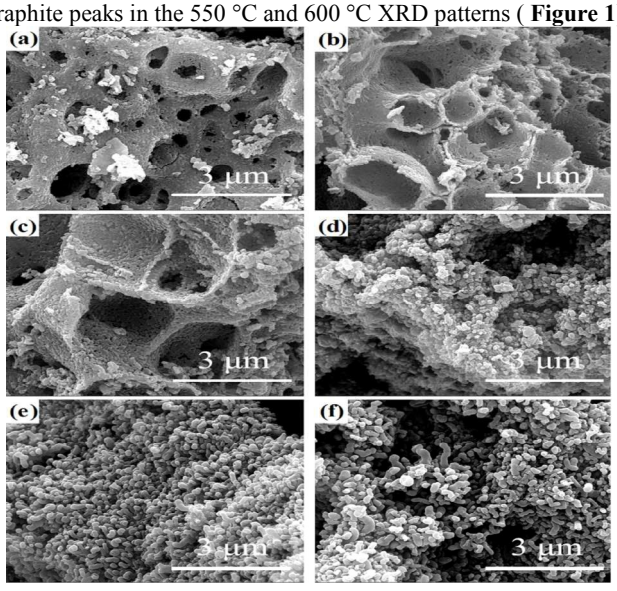

Figure 2. SEM images of (a) $BaFe_{12}O_{19}$ and the $BaFe_{12}O_{19}$/Fe_3C/CNTs composites obtained at (b) 400 °C, (c) 450 °C, (d) 500 °C, (e) 550 °C and (f) 600 °C.

TEM images of $BaFe_{12}O_{19}/Fe_3C$/CNTs composites synthesized at 600 °C are shown in **Figure 3**. It can be observed that the straight CNTs have a quasi-linear structure with outer diameter and inner diameter range of 75-95 nm and 25-45 nm, respectively. The magnetic catalyst particles locating in the tip of the carbon nanotubes are sphere-like with a diameter of 20-80 nm (**Figure 3**c). Furthermore, the lattice fringes of catalyst particles can be seen clearly, by accurate measurement of the HRTEM image of the catalyst particles, its lattice fringes spacing are determined to be 0.21 nm and 0.28 nm, which are consistent with the (211) diffraction peak of Fe_3C and (110) diffraction peak of $BaFe_{12}O_{19}$ respectively. The lattice distance of the outer layer structure is 0.36 nm, corresponding to the (002) plane of graphite, in good agreement with the XRD analysis (**Figure 3**d).

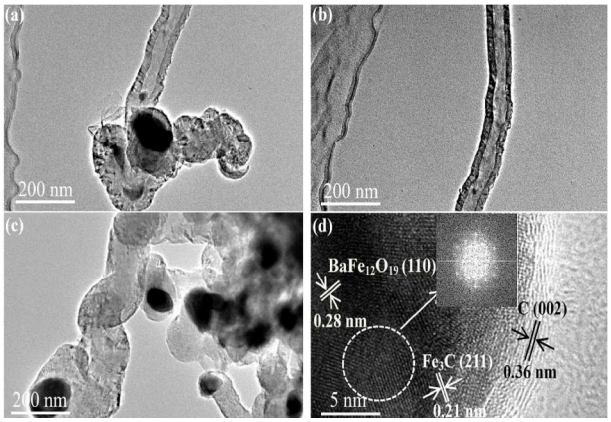

Figure 3. TEM images of $BaFe_{12}O_{19}/Fe_3C$/CNTs composites synthesized at 600 °C.

Figure 4a, **4**b show the real and imaginary part of the complex dielectric permittivity (ε' and ε'') for pure $BaFe_{12}O_{19}$ porous particles and the composites synthesized at 400-600 °C in 2-18 GHz frequency range. It is found that the ε' for raw $BaFe_{12}O_{19}$ is nearly about 2.3 and the ε'' is almost zero, indicating that the dielectric losses of $BaFe_{12}O_{19}$ are very poor.[14] For the $BaFe_{12}O_{19}/Fe_3C$/CNTs composites synthesized at 400-600 °C the value of the complex dielectric permittivity decrease with increasing frequency in the 2-18 GHz range as shown in **Figure 4**a. However, for the composites synthesized at 550 °C, the real part of relative permittivity increases from 9.0 to 11.2 over a range of 2-10 GHz, and decreases slowly to 9.8. It is reported that dielectric constant and dielectric loss in the composite depend on the three main factors: temperature, frequency and MWNT concentration.[15] Except for the temperature (determine the intrinsic conductivity) and frequency, the carbon concentration play a major role in adjusting the dielectric feature. In our experimental system, the length and content of the carbon nanotubes (CNTs) increase with the temperature increasing. It is found that the 550 °C product has highest ε''. We suggest that excessive temperature leads to the change in morphology and microstructure of the carbon nanomaterials.[16] And dielectric constant and dielectric loss decrease may due to some defect structure resulting in relatively low conductively in case of 600 °C. Moreover, the composites possesses a higher ε'' value than pure $BaFe_{12}O_{19}$ nanoparticles due to the introducing of CNTs to enhance electric polarization.[17] And according to the free electron theory, $\varepsilon'' \approx 1/(2\pi\varepsilon_0\rho f)$, the higher ε'' value means a lower electric resistivity.[18] For the tan δ_ε curve, all the such composites synthesized at 400-600 °C perform high dielectric loss values, and the distinct dielectric loss properties mainly arise from free electrons in the composites.[19] It is obvious that the tan δ_ε values of 500-550 °C samples are higher than that of 600 °C samples as shown in **Figure 4**e. However, too high dielectric loss results in poor matching of the dielectric loss and magnetic loss, leading to a relatively poor microwave absorbing.[20] Apparently, a reasonable dielectric loss for the 600 °C samples could make a better microwave absorbing performance.[21]

The EDX result of $BaFe_{12}O_{19}/Fe_3C$/CNTs composites obtained at 450-600 °C demonstrates the existence of C, O, Ba and Fe elements. According to EDX report, the atomic ratio of C in composites synthesized at 450 °C, 500 °C, 550 °C and 600 °C are 0.48%, 1.27%, 25.91% and 54.84% respectively. Then the content of carbon is increasing with the increase of the temperature. And the dielectric losses in the composites are attributed to the CNTs, so the dielectric losses mainly increase with elevated temperature except 600 °C sample with defect structure formed at excessive temperature. (Figure S1 and Table S1 in the Supporting Information).

The complex permeability (μ' and μ'') results of pure $BaFe_{12}O_{19}$ and such composites are depicted in **Figure 4**c, **4**d. The real part of the permeability in both pure $BaFe_{12}O_{19}$ and interrelated composites are almost constant. And the 550 °C composites possess the relatively higher imaginary part of the permeability than other composites and pure $BaFe_{12}O_{19}$. From tan δ_μ curve in **Figure 4**f, it can be observed that the products synthesized at 550 °C possess the highest tan δ_μ value, the maximum value of the magnetic tangent loss of the 550 °C composites reaches 0.45. However, too high ε'' lead to weak microwave absorbing properties of the 550 °C composites .[22]

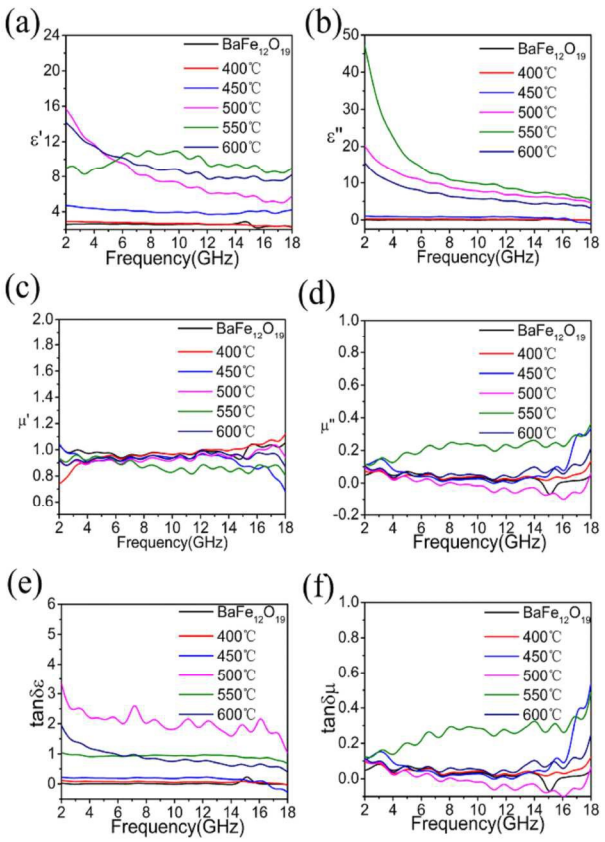

Figure 4. Measured relative (a, b) complex permittivity, (c, d) complex permeability and (e, f) dielectric and magnetic loss values of original $BaFe_{12}O_{19}$ nanoparticles and the $BaFe_{12}O_{19}/FeC_3$/CNTs composites synthesized at the range of 400-600 °C.

The reflection loss (RL) coefficients of the above materials are calculated from the measured experimental values. Using the data of

complex permittivity and permeability, based on the transmission theory, the reflection loss (RL) can be calculated from the equations shown below.

$$R_L=20\log\left|\frac{Z-1}{Z+1}\right| \quad (1)$$

$$Z = (\mu_r / \varepsilon_r)^{1/2} \tanh [j(2\pi fd/c)(\mu_r \varepsilon_r)^{1/2}] \quad (2)$$

where f is the microwave frequency, d is the thickness of the absorber, c is the velocity of light and Z is the input of the absorber.[23] The impedance matching condition is determined by the combinations of six parameters (namely, ε', ε'', μ', μ'', f and d). The reflection loss curve versus frequency can be calculated from μ_r and ε_r at an as-designed layer thickness.

Figure 5 shows the calculated RL curves over the 2-18 GHz frequency range for pure $BaFe_{12}O_{19}$ and the products synthesized at 400-600 °C with a thickness of 2.5 mm. It can be seen that the microwave absorption properties of the pure $BaFe_{12}O_{19}$ performs poor behavior for electromagnetic loss with RL values more than -4.7 dB. The products obtained at 400-550 °C show a little better behavior for electromagnetic loss at 2-18 GHz frequency, due to its higher dielectric loss and lower loss magnetic compared with pure $BaFe_{12}O_{19}$. The 600 °C composite shows the minimum RL of -12.1 dB, and have an interval width of 3.1 GHz with losses below -10 dB from 8.2 to 12.3 GHz. As shown in **Figure 6**, the minimum RL value of $BaFe_{12}O_{19}$ is -4.7dB at 15GHz, and the minimum RL values of composites synthesized at 400 °C, 450 °C, 500 °C, 550 °C and 600 °C are -2.5 dB, -7.9 dB, -10.8 dB, -8.4 dB, -14.75dB at 16.5GHz, 16.2 GHz, 12 GHz, 11.82 GHz, 10.3 GHz, respectively. Besides, the minimum reflection loss shifts toward lower frequency with increasing sample thickness, which indicates that the range of absorption frequency can be modulated by adjusting the thickness of the composites.[24] Materials with RL values of less than -10 dB absorption are considered to be suitable EM wave absorbers,[25] the $BaFe_{12}O_{19}$ nanoparticles and the products synthesized at 400 °C, 450 °C and 550 °C show relatively poor behavior for electromagnetic loss. The reason is that the attenuation mechanism of those samples are mainly based on either dielectric loss or magnetic loss, and only magnetic loss or dielectric loss leads to weak EM attenuation.[26] And the products obtained at 500 °C and 600 °C exhibit improvement in electromagnetic wave loss due to a moderate value of ε''-μ''. It is suggested that too high ε'' (composite obtained at 550 °C) results in too much reflection, relatively low ε'' ($BaFe_{12}O_{19}$, composites obtained at 400 °C and 450 °C) lacks dielectric loss ability, and a moderate ε'' leads to better absorption properties.

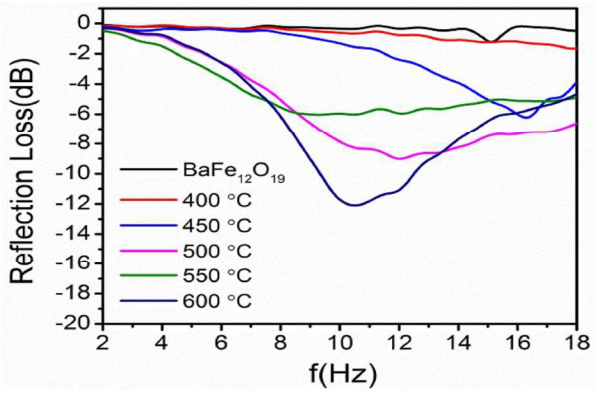

Figure 5. Microwave RL curves of samples (pure $BaFe_{12}O_{19}$ nanoparticles and $BaFe_{12}O_{19}/FeC_3$/CNTs composites)–wax composites (mass ratio=3:7) of 2.5 mm at 2–18 GHz.

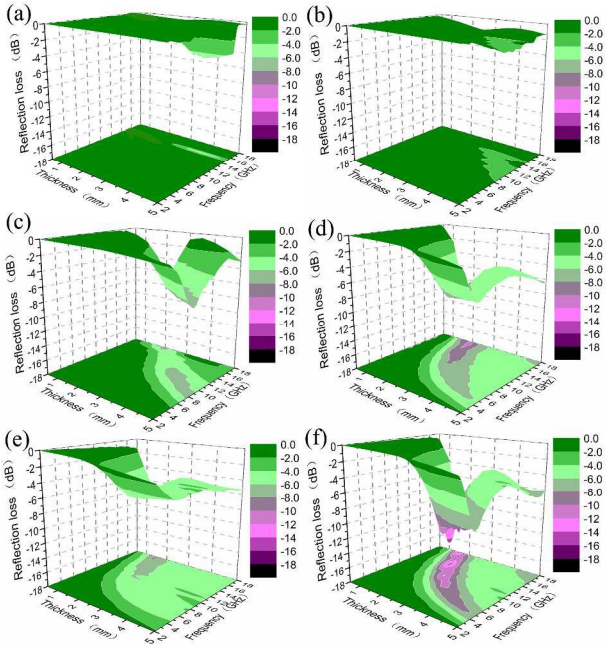

Figure 6. Simulated curves of electromagnetic wave loss of (a) $BaFe_{12}O_{19}$ and the $BaFe_{12}O_{19}/Fe_3C$/CNTs composites when the temperature is (b) 400 °C, (c) 450 °C, (d) 500 °C, (e) 550 °C and (f) 600 °C.

Conclusion

A series of $BaFe_{12}O_{19}/Fe_3C$/CNTs composites are synthesized using acetylene CVD at 400-600 °C. The temperature holds host to the formation and structure of the obtained composites. The CNTs among composites grow well at reaction temperatures ranging from 450 °C to 600 °C. The reflection loss of pure $BaFe_{12}O_{19}$ is mainly due to magnetic loss, while the $BaFe_{12}O_{19}/Fe_3C$/CNTs composite obtained at 450-550 °C is mainly attributed to dielectric loss. The 600 °C sample performs an improved microwave absorbing behavior because of its $BaFe_{12}O_{19}/Fe_3C$/CNTs composites structure leading to well match between the dielectric and magnetic loss.

Acknowledgements

This work was financially supported by the National Natural Science Foundation of China (Grant No. 51402040, 51302029) and the Open Foundation of State Key Laboratory of Electronic Thin Films and Integrated Devices (KFJJ201411).

Notes and references

[1] School of Energy Science and Engineering, State key Laboratory of Electronic Thin Films and Integrated Devices, Center for Information in Biomedicine, University of Electronic Science and Technology of China, Chengdu, 611731, China

[2] Research Center for Eco-Environmental Sciences, Chinese Academy of Sciences, Beijing, 100085, China

[3] Key laboratory of Magnetic Levitation Technologies and Maglev Trains (Ministry of Education of China), Superconductivity and New Energy Center (SNEC), Southwest Jiaotong University; Chengdu, Sichuan 610031, China

[ξ] Liangjun Yin, Tong Chen and Shiyu Liu contributed equally to this work.

[*] Corresponding Author: Email: jianxian@uestc.edu.cn and xzhang@my.swjtu.edu.cn

1. K. Khan, *Journal of Superconductivity and Novel Magnetism*, 2013, **27**, 453-461.
2. X. Huang, J. Zhang, M. Lai and T. Sang, *Journal of Alloys and Compounds*, 2015, **627**, 367-373.
3. L. Li, K. Chen, H. Liu, G. Tong, H. Qian and B. Hao, *Journal of Alloys and Compounds*, 2013, **557**, 11-17.
4. A. Mali and A. Ataie, *Scripta Materialia*, 2005, **53**, 1065-1070.
5. H. He, F. Luo, N. Qian and N. Wang, *Journal of Applied Physics*, 2015, **117**, 085502.
6. L. Hongfei, W. Jianjiang, X. Baocai and L. Zhiguang, *Journal of Materials Science: Materials in Electronics*, 2015.
7. P. Liu and Y. Huang, *RSC Advances*, 2013, **3**, 19033.
8. X. Yang, Z. Wang, M. Jing, R. Liu, F. Song and X. Shen, *Ceramics International*, 2014, **40**, 15585-15594.
9. T.-H. Ting and K.-H. Wu, *Journal of Magnetism and Magnetic Materials*, 2010, **322**, 2160-2166.
10. H. Sözeri, Z. Mehmedi, H. Kavas and A. Baykal, *Ceramics International*, 2015.
11. H. Lin, H. Zhu, H. Guo and L. Yu, *Materials Letters*, 2007, **61**, 3547-3550.
12. L. Kong, X. Yin, X. Yuan, Y. Zhang, X. Liu, L. Cheng and L. Zhang, *Carbon*, 2014, **73**, 185-193.
13. J. Zhao, Y. Xie, Z. Le, Y. Luo, Y. Gao, R. Zhong, Y. Qin, J. Pan and Y. Huang, *Polymer Composites*, 2013, **34**, 1801-1808.
14. L. W. Jiang, Z. H. Wang, D. Li, Y. Wang , W. Liu and Z. D. Zhang, *RSC Advances*, 2015, **5**, 40384.
15. W. Song, M. Cao, Z. Hou, J. Yuan and X. Fang, *Scripta Materialia*, 2009, **61**, 201-204.
16. X. Jian, M. Jiang, Z. W. Zhou and M. L. Yang, *ACS Nano*, 2012, **10**, 8611-8619.
17. Y. B. Feng, T. Qiu and C. Y. Shen, *Journal of Magnetism and Magnetic Materials*, 2007, **318**, 8-13.
18. M. R. Meshram, N. K. Agrawal, B. Sinha and P. S. Misra, *Journal of Magnetism and Magnetic Materials*, 2004, **271**, 207-214.
19. Z. Fan, G. Luo, Z. Zhang, L. Zhou and F. Wei, *Materials Science and Engineering: B*, 2006, **132**, 85-89.
20. A. Ghasemi, A. Hossienpour, A. Morisako, A. Saatchi and M. Salehi, *Journal of Magnetism and Magnetic Materials*, 2006, **302**, 429-435.
21. H. L. Lu, A. B. Zhang, Y. P. Zhang and L. C. Ding, *RSC Advances*, 2013, **00**, 1-3.
22. X. Y. Lu, Y. Z. Wu, , L. M. Ni, and L. Jiang, *RSC Advances*, 2015, **5**. 54175.
23. A. Ghasemi, A. Hossienpour, A. Morisako, X. Liu and A. Ashrafizadeh, *Materials & Design*, 2008, **29**, 112-117.
24. W. Jing, Z. Hong, B. Shuxin, C. Ke and Z. Changrui, *Journal of Magnetism and Magnetic Materials*, 2007, **312**, 310-313.
25. G. Mu, N. Chen, X. Pan, H. Shen and M. Gu, *Materials Letters*, 2008, **62**, 840-842.
26. A. N. Yusoff and M. H. Abdullah, *Journal of Magnetism and Magnetic Materials*, 2004, **269**, 271-280.